RESEARCH/REVIEW ARTICLE

Assessing trend and variation of Arctic sea-ice extent during 1979–2012 from a latitude perspective of ice edge

Wentao Xia,[1] Hongjie Xie[1] & Changqing Ke[2]

[1] Laboratory for Remote Sensing and Geoinformatics, Department of Geological Sciences, University of Texas at San Antonio, San Antonio, TX 78249, USA
[2] School of Geographic and Oceanographic Sciences, Nanjing University, Nanjing, 210093, China

Keywords
NSIDC ice index; Arctic; sea-ice extent; ice-edge latitude.

Correspondence
Hongjie Xie, Laboratory for Remote Sensing and Geoinformatics, Department of Geological Sciences, University of Texas at San Antonio, San Antonio, TX 78249, USA.
E-mail: hongjie.xie@utsa.edu

Abstract

Arctic sea-ice extent (in summer) has been shrinking since the 1970s. However, we have little knowledge of the detailed spatial variability of this shrinking. In this study, we examine the (latitudinal) ice extent along each degree of longitude, using the monthly Arctic ice index data sets (1979–2012) from the National Snow and Ice Data Center. Statistical analysis suggests that: (1) for summer months (July–October), there was a 34-year declining trend in sea-ice extent at most regions, except for the Canadian Arctic Archipelago, Greenland and Svalbard, with retreat rates of 0.0562–0.0898 latitude degree/year (or 6.26–10.00 km/year, at a significance level of 0.05); (2) for sea ice not geographically muted by the continental coastline in winter months (January–April), there was a declining trend of 0.0216–0.0559 latitude degree/year (2.40–6.22 km/year, at a significance level of 0.05). Regionally, the most evident sea-ice decline occurred in the Chukchi Sea from August to October, Baffin Bay and Greenland Sea from January to May, Barents Sea in most months, Kara Sea from July to August and Laptev Sea and eastern Siberian Sea in August and September. Trend analysis also indicates that: (1) the decline in summer ice extent became significant (at a 0.05 significance level) since 1999 and (2) winter ice extent showed a clear changing point (decline) around 2000, becoming statistically significant around 2005. The Pacific–Siberian sector of the Arctic accounted for most of the summer sea-ice decline, while the winter recovery of sea ice in the Atlantic sector tended to decrease.

Sea ice covers vast areas in the Arctic Ocean, blocks or limits heat exchange between ocean water and atmosphere, has a much higher surface albedo than sea water, and plays an important role in the thermohaline circulation. Thus, Arctic sea ice significantly affects Northern Hemisphere climate and ocean circulation (Mauritzen & Häkkinen 1997; Perovich et al. 2002). On the other hand, Arctic sea ice is sensitive to changes of air temperature and prone to wind forcing and oceanic circulation (Rigor et al. 2002; Ogi & Wallace 2007), responding to climate change with changes in ice thickness, age and extent.

Sea-ice extent is commonly defined as the area where the sea-ice concentration is greater than 15%; this boundary is defined as the ice edge (Parkinson & Cavalieri 2008). Arctic sea-ice extent has a strong seasonal cycle and reaches its maximum extent in March and minimum in September of each year (Parkinson et al. 1999; Eisenman 2010). In winter, there is little inter-annual difference in ice extent, while the summer ice extent has been declining in recent years (Chapman & Walsh 1993; Vinnikov et al. 1999; Hansen et al. 2006; Hansen et al. 2010; Shakun et al. 2012; Parkinson & Comiso 2013). During the freezing months, oceanic heat can be quickly lost to the atmosphere due to the lack of an insulating ice cover, after the low summer minimum. This forms a long-wave negative feedback, which effectively mitigates the weakened

Citation: *Polar Research* 2014, *33*, 21249, http://dx.doi.org/10.3402/polar.v33.21249

ice-albedo feedback and leads to the rapid expansion of sea-ice extent (Tietsche et al. 2011). However, this has not stopped the declining trend: ice age and ice thickness have been constantly decreasing in recent years (Perovich 2011; Jeffries et al. 2013; Xie et al. 2013).

Since the 1970s, satellite passive microwave remote sensing has routinely monitored the sea-ice extent across the entire Arctic Ocean. The trend of summer sea-ice extent decline is −2.8%/decade during 1978–1996, −3.7%/decade during 1979–2006, and −4.1%/decade during 1979–2010. The rapid decline is mostly attributed to Arctic warming, ice-albedo feedback (Comiso 1986; Parkinson et al. 1999; Parkinson & Cavalieri 2008; Cavalieri & Parkinson 2012) and atmospheric circulation anomalies such as the Arctic Dipole Anomaly (Wang et al. 2012). In recent decades, dynamic processes like wind forcing have played a minor role in the recently recorded minimum ice extent events (Zhang et al. 2013). Southerly wind and intense summer cyclone activity contributed much to massive sea-ice loss in 2002 (Serreze et al. 2003) and 2007 (Overland et al. 2008; Zhang et al. 2008; Zhang et al. 2012; Zhang et al. 2013). The overall thinned Arctic ice-pack—resulting from the abnormally low Arctic perennial ice coverage in recent years—is much more susceptible to such dynamic processes (Comiso et al. 2008).

In addition to microwave remote sensing, analyses of reconstructed historical data sets that predate the satellite era have also suggested a long-term declining trend of Arctic sea-ice extent in the past 80–150 years (Divine & Dick 2006; Mahoney et al. 2008), as sea-ice decline associated with warming was found in the Nordic seas and the Russian Arctic. Models analysing the thermodynamic and dynamic processes associated with Arctic sea-ice decline have simulated the development of sea-ice conditions. The coupled simulations of the Pan-Arctic Ice-Ocean Modelling and Assimilation System (Zhang & Rothrock 2003; Zhang et al. 2012) presented a substantial Arctic sea-ice volume loss due to increasing surface air temperature and a 37% reduction in the mechanical strength of the thinner ice during 1979–2011. The Coupled Climate Model simulation predicted that an ice-free Arctic summer is expected in the 2050s instead of 2100s (Holland et al. 2010).

Previously, sea-ice extent and its changes were interpreted by examining ice extent across the entire Arctic or in each subsector (Parkinson et al. 1999; Parkinson & Cavalieri 2008; Cavalieri & Parkinson 2012). Mostly focused on the summer minimum mean ice extent, such studies have paid less attention to the ice extent in other seasons. Analysis of the spatial variations in each region is also lacking. Eisenman (2010) assessed sea-ice extent changes by looking at the zonal averaged latitudes that the Arctic ice-pack reached over different longitudes. This new method can detail the seasonal/inter-annual variation, trend and spatial patterns of the sea-ice extent. This paper further develops Eisenman's approach by applying the trend analysis to latitudinal ice edge along each degree of longitude, to gain a more detailed understanding of the 34-year Arctic sea-ice extent changes from 1979 to 2012.

Data and method

National Snow and Ice Data Center ice index

The National Snow and Ice Data Center (NSIDC) ice index (Fetterer 2002–2012) is a series of data sets generated from the US Defense Meteorological Satellite Program's Special Sensor Microwave/Imager (DMSP SSM/I) and Scanning Multichannel Microwave Radiometer (SSMR) Nimbus-7 passive microwave data, providing consistent and up-to-date information about sea-ice concentration and extent changes (Campbell et al. 1980; Eisenman 2010; Fetterer et al. 2004; Meier et al. 2005). The data sets mainly include: (1) monthly mean sea-ice extent and area; (2) monthly sea-ice extent anomalies with trend lines and significance intervals; and (3) sea-ice extent (with an outline of the median extent for that month for comparison), sea-ice concentration, trends in sea-ice concentration and anomalies in sea-ice concentration (the NSIDC calculated these areal anomalies and median extents based on the reference period from 1979 to the present).

As the data source, Nimbus-7 SSMR and DMSP SSM/I have been frequently used for large-scale sea-ice monitoring (Cavalieri et al. 1984; Hollinger et al. 1990; Emery et al. 1994). The accuracy of the derived sea-ice index products is highly dependent on the accuracy of sea-ice concentration derived from passive microwave sensed brightness temperatures in different channels. As the NSIDC sea-ice index uses the National Aeronautics and Space Administration Team algorithm (Cavalieri et al. 1984) to estimate ice concentration, its accuracy depends on the type of sea ice being imaged (Gloerson & Campbell 1991). When the sea ice is thin, the algorithm is less reliable; in addition, the passive microwave sensor itself cannot reliably distinguish melt ponds and isolated floes (Cavalieri et al. 1984). Compared with synthetic aperture radar data and ice charts from operational ice centres (Kwok 2002; Partington et al. 2003), the passive microwave data underestimate sea-ice area and concentration during the spring and summer seasons (Comiso & Kwok 1996; Fetterer & Untersteiner 1998).

A 15% ice concentration threshold is commonly applied to identify the ice edge. This threshold can remove the

Citation: *Polar Research* 2014, *33*, 21249, http://dx.doi.org/10.3402/polar.v33.21249

uncertainty caused by low ice concentration, thin ice thickness and atmospheric interference (Fetter 2002; Parkinson & Cavalieri 2008). In addition, it also reduces the confusion between ice-pack and isolated small ice floes (Parkinson & Cavalieri 2008).

Since 19 June 2002, the Advanced Microwave Scanning Radiometer for the Earth Observing System (AMSR-E) onboard the Aqua satellite provides daily sea-ice concentration products with 12.5 km spatial resolution. Comparison in this study found that if the same 15% ice concentration threshold is applied to the AMSR-E ice concentration product, the resulting monthly median ice edge from AMSR-E is very much similar to the NSIDC ice index, primarily based on SSM/I and SSMR. During 2003–2011, ice-pack area difference between these two products is always less than 30 000 km^2 (or 5%). This is particularly seen in summers when passive microwave remote sensing has the highest uncertainty. The minor differences between the two ice edges are mostly due to the different spatial resolutions. In addition, due to the antenna malfunction of AMSR-E, no further sea-ice concentration products of AMSR-E have been available since 3 October 2011. The only nine-year AMSR-E sea-ice concentration time series is not sufficient for a long-term trend analysis.

Retrieving latitudinal ice edge

The monthly ice-edge data (shapefile) of the NSIDC ice index data sets from January 1979 to December 2012 were used to retrieve the latitudinal ice edges. The latitudes on the intersect points of ice edge at each integer degree of longitude were extracted. Where there were several intersect points, only the southernmost points of the ice-pack edge along each longitude degree were considered. Tiny ice floes and isolated land fast ice were ignored.

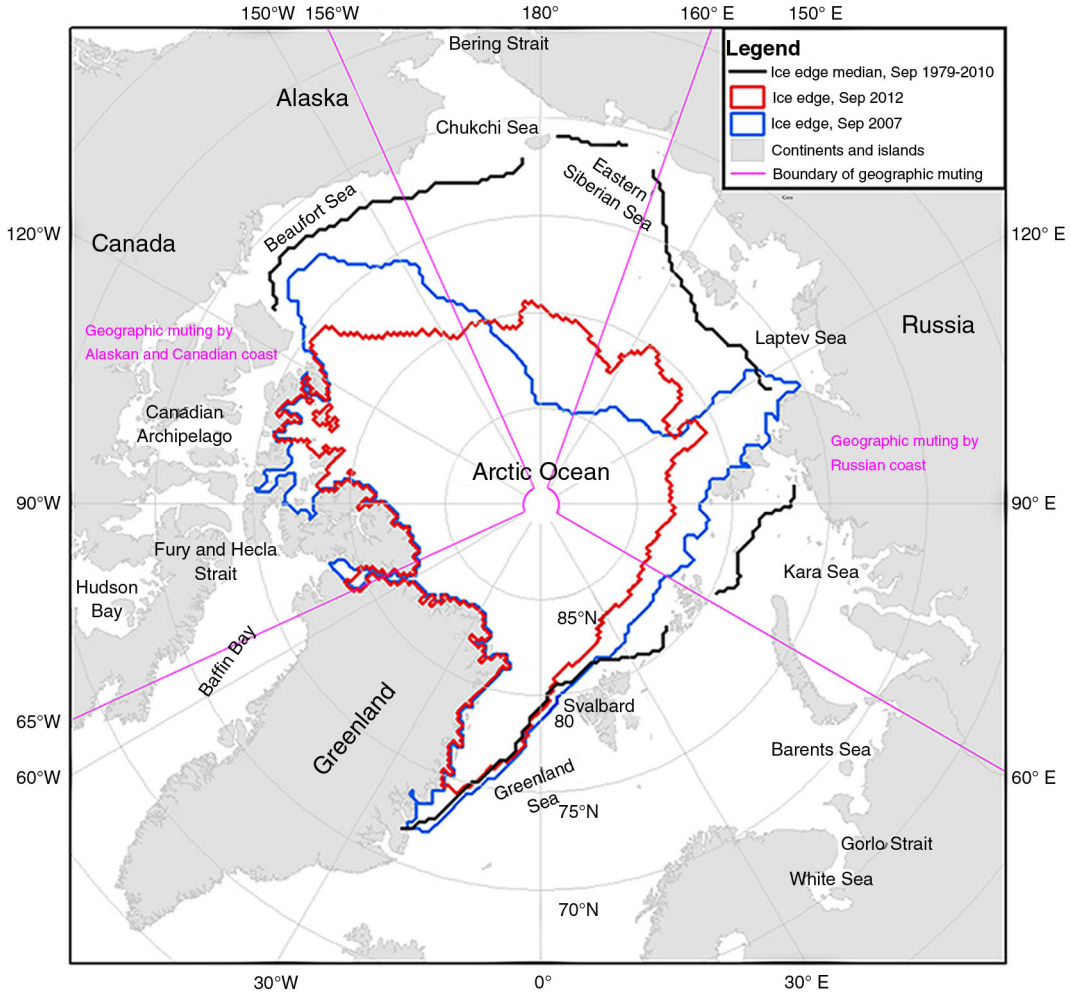

Fig. 1 Geography of the Arctic Ocean, marginal seas and continental coast, with three representative ice edges from the National Snow and Ice Data Center ice index (geographically muted areas excluded in analysis for winter months only).

Geographic muting of fall/winter sea-ice expansion

The fall/winter expansion of ice extent can eventually be blocked by the continental coast (Fig. 1). This has been referred to as geographic muting (Eisenman 2010). To determine if ice extent on certain longitudes was confined by the continental coast in winter, the position of the continental coast and ice edge were compared. If the difference between maximum and minimum latitudinal ice edges is less than 1 degree and the distance between ice edge and continental coast is less than 1 degree in winter, the geographic muting is in effect at this longitude degree. From 65° W to 156° W (Beaufort Sea), sea-ice expansion is geographically muted by the Alaskan and Canadian coasts. From 60° E to 160° E (Barents, Kara and Laptev seas), sea-ice expansion is geographically muted by the European and Russian coasts. Greenland does not geographically mute the winter sea-ice expansion, because sea ice can expand to the south of the island. When these criteria are applied, longitude or directions where sea-ice winter expansion is not geographically muted can be found. In this paper, analysis of the winter sea-ice extent is only focused on areas which are not affected by such muting to address the potential change of the winter ice edge.

Data analysis and comparison

Three-dimensional surface plots are used to represent the ice-edge latitude anomalies and trends. The anomalies stated here are the differences between the actual ice-edge latitude and monthly/latitudinal averaged ice-edge latitude. The trend is represented by the slope of the linear regression (with a 95% confidence interval). If the lower bound of the 95% confidence interval is greater than 0, the trend is significant (at a 0.05 significance level). A significant positive trend indicates that the ice-edge latitude is increasing (or retreating northward), and the ice extent is decreasing. In addition, if the margin of error of the slope (numerical difference between upper bound and lower bound of the confidence interval) is negligible compared to the value of the slope, the uncertainly is low. Therefore, the trend is assured (Cavalieri & Parkinson 2012).

With the 34 years (1979–2012) of ice extent data, the changing point of the slope can be analysed using the Mann–Kendall (M–K) procedure (Mann 1945; Kendall 1955). This is a non-parametric test often used in meteorology and hydrology studies to detect trends in a time series. The null hypothesis of this test states that the data samples are independent and randomly distributed. Rejection of the null hypothesis indicates the existence of a trend, or correlation between this series of data. Besides the trend, the changing point of the trend can also be detected by this procedure.

The M–K statistics (d_k) is calculated from a time series of N observations, whose value can be denoted as $x_1, x_2, \ldots, x_N$ (*1,2,...,N* is the order in the time series), and m_i is the count that $\boldsymbol{x_j} > \boldsymbol{x_i}$ $(1 \le j \le i)$ for the *i*th sample x_i. The equation is:

$$d_k = \sum_{i=1}^{k} m_i, (2 \le k \le N) \tag{1}$$

Assuming the null hypothesis is true and the time series is randomly independently distributed, d_k is normally distributed, and the mean of the d_k is:

$$E[d_k] = \frac{k(k-1)}{4}, (2 \le k \le N), \tag{2}$$

the variation of the d_k is:

$$Var(d_k) = \frac{k(k-1)(2k+5)}{72}, (2 \le k \le N), \tag{3}$$

and the normalized d_k is:

$$u(d_k) = \frac{d_k - E[d_k]}{\sqrt{Var(d_k)}}, (2 \le k \le N), \tag{4}$$

and $u(d_k)$ follows the standard normal distribution $(u(d_k) \sim N(0,1))$.

This $u(d_k)$ is one of the M–K statistics describing the likelihood that all samples of the time series are independently and randomly distributed. If $|u(d_k)| < u(d_k)_\alpha$, where α denotes the significance level, the null hypothesis cannot be rejected and no trend can be concluded. If $|u(d_k)| > u(d_k)_\alpha$, where α denotes the significance level, the null hypothesis is rejected and the trend is very likely to be significant. As the upper and lower boundaries of the 95% confidence interval of $u(d_k)_\alpha$ is ± 1.96, if the $|u(d_k)| > 1.96$, the trend is significant at a 0.05 significance level.

The next step is to calculate $u(d_k)$ statistics from a reverse order. Let m'_i be the count that $x_j > x_i$ $(i \le j \le N)$ for x_i and $u'(d_k)$ calculated from this m'_i, as:

$$d'_k = \sum_{i=1}^{k} m'_i, (2 \le k \le N) \tag{5}$$

Similarly,

$$u(d'_k) = \frac{d_k - E[d'_k]}{\sqrt{Var(d'_k)}} (2 \le k \le N) \tag{6}$$

The values of $u(d_k)$ and $u(d'_k)$ can be plotted as a curve by value k $(1 \le k \le N)$. The point where $u(d_k)$ exceeds the value of $u(d_k)_{0.05}$ is the point on the time series that the trend becomes significant at a 0.05 significance level. If the $u(d_k)$ and $u(d'_k)$ curves cross each other and the value of the crossing point ranges between 0 ± 1.96, this point is a changing point of the trend.

Citation: *Polar Research* 2014, *33*, 21249, http://dx.doi.org/10.3402/polar.v33.21249

Results

The averaged winter (January–April) and summer (July–October) mean ice-edge latitudes of the 34 years (Fig. 2) indicate that: (1) in winter, the ice extended across the Arctic marginal seas, expanded to the Bering Sea, Hudson Bay and the White Sea and reached the coasts of Alaska, Canada, Europe and Russia; (2) in summer, the ice edge retreated markedly from the Bering Sea, Canadian Arctic Archipelago, Hudson Bay, Baffin Bay and the Greenland, Barents and Kara seas. It should be noted that the 2012 minimum extent significantly differed from the 2007 minimum, except for around Greenland.

In June, the sea ice covered Hudson Bay. Later in July and August, there were only isolated ice floes and fast ice left in Hudson Bay. The June ice index maps sometimes misclassify the sea ice within the Fury and Hecla Strait, which links the Arctic Ocean to Hudson Bay, as open water, so the ice edge is mapped to the north of the strait, not in Hudson Bay. This misclassification error is caused by the large pixel size of passive microwave imagery and the narrow width of the strait.

Ice-edge variation over 34 years

Figure 3 shows the ice extent anomalies in latitude degree to the 34-year mean for the 1979–2012 period, for both winter months and summer months. A positive anomaly indicates a northward shift in the ice edge, i.e., the ice is retreating or declining. In winter months, ice extent in the Beaufort Sea, Canadian Arctic Archipelago, Hudson Bay, Baffin Bay, Kara Sea and Laptev Sea did not have any significant inter-annual variation. After 1999, Greenland was no longer surrounded by sea ice in winter, as shown in Fig. 3a, where more and more red around 50°W (−50°) longitude, indicates ice-edge retreat. Sea ice in the western part of the Barents Sea, around 30°–40°E, was advancing (blue in the figure), before it consistently declined (red in the figure) in the last decade. Sea ice in the eastern part of the Barents Sea, around 40°–60°E, did not show much change. Sea-ice edge on the Bering Sea sector (and the Gulf of Anadyr) had a high inter-annual variation in winter and a decreasing trend in summer.

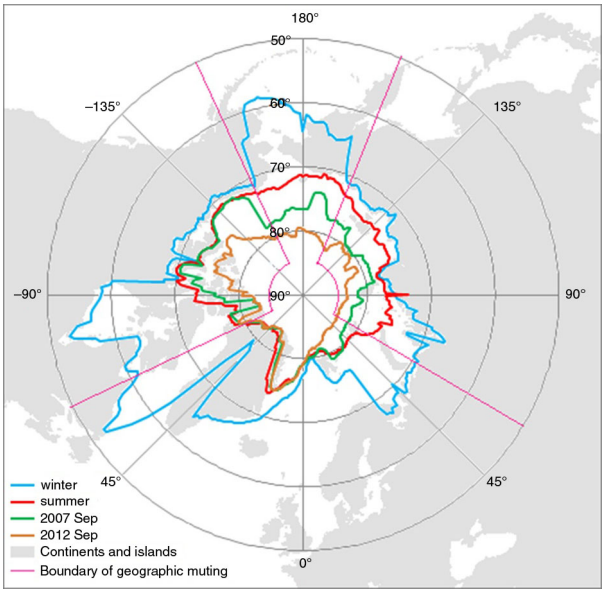

Fig. 2 Thirty-four-year averaged latitudinal ice edges in winter (January–April) and summer (July–October) months from 1981 to 2012, compared with the summer minimums of 2007 and 2012.

No obvious summer declining trend can be seen before 2000. Since 2002, however, the northward shifting occurred at almost all longitudes, with only a few exceptions in a few years. The 5 degree northward shift occurred at most longitudes in 2012, especially in eastern Siberian Sea, Kara Sea, Beaufort Sea and Chukchi Sea. This means that the decline was much more evident in the Pacific–Siberian sector (including Beaufort Sea, Bering Sea/Chukchi Sea, eastern Siberian Sea and Laptev Sea) of the Arctic Ocean and less evident in the Atlantic sector (including Hudson Bay, Baffin Bay, Greenland, Greenland Sea, Svalbard, Barents Sea and Kara Sea), especially in Greenland and Svalbard.

Changes in seasonal cycle of latitudinal ice extent

Comparing seasonal cycle based on five-year periods. Figure 4 shows the five-year averaged ice-edge latitudes in each month, compared with the 34-year (1979–2012) mean. The 2007 and 2012 ice extents are plotted individually. In the four winter months (January–April), the latitudinal ice edges were similar. The 2007 winter ice edge was located considerably north in Baffin Bay, the Greenland, Barents and eastern Siberian seas, compared to other years (not shown). In the melting months (May and June), the rate of melting gradually increased from the earliest five-year period (1981–85) to the latest five-year period (2006–2010). The September ice edge during 2006–2010 was 1.29 degrees further north than the 34-year mean. The freezing months (November and December) tended to have a higher ice recovery rate during the years 2006–2010. The northward shift of ice edge in 2007 and 2012 was the fastest, and the winter expansion/recovery was much more rapid compared to other years.

In the fall, the ice tended to recover rapidly and reach a similar maximum extent in March. Faster ice-edge expansion since 2007 should be mostly attributed to a stronger long-wave negative feedback following the summer minimum (Tietsche et al. 2011). This rapid ice

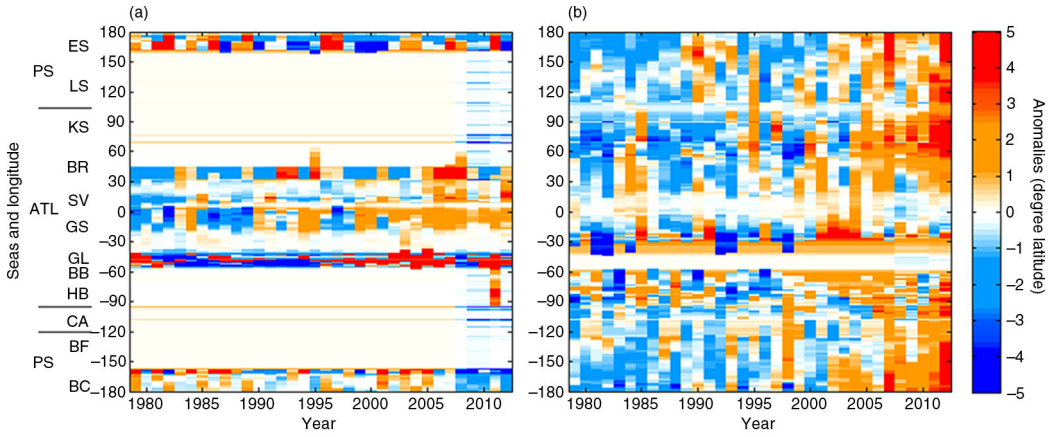

Fig. 3 Ice extent anomalies in latitude (degree) over each longitude for (a) the winter months of January–April and (b) the summer months of June–October from 1979 to 2012. The following terms are abbreviated: eastern Siberian Sea (ES); Laptev Sea (LS); Kara Sea (KS); Barents Sea (BR); Svalbard (SV); Greenland Sea (GS); Greenland (GL); Baffin Bay (BB); Hudson Bay (HB); Canadian Arctic Archipelago (CA); Beaufort Sea (BF); Bering Sea/Chukchi Sea (BC); Pacific–Siberian sector (PS) and Atlantic sector (ATL).

expansion does not mitigate the loss of sea-ice volume, since the new ice is thin and fragile, susceptible to dynamic forcing induced by wind and oceanic current anomalies. Since most of the seasonal ice does not survive the next summer, replenishment of multiyear ice is hindered (Perovich 2011). In addition, the existing multiyear ice is also thinning and is prone to transpolar drift (Haas et al. 2008). As the Arctic has been consistently warming in recent decades, the thermodynamic forcing that has contributed to Arctic sea-ice loss is also strengthening (Gillett et al. 2002; Comiso 2003).

Per-longitude comparison of seasonal cycle to mean level. Seasonal cycles of latitudinal ice extent are compared to the 34-year mean level along each direction (i.e., an integer degree of longitude), with the same five-year period used in Fig. 4. The five-year periods of

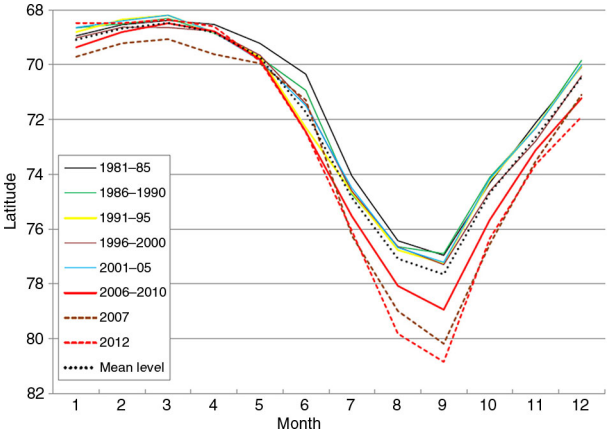

Fig. 4 Five-year averaged seasonal cycle of latitudinal ice extent with the 34-year mean, and the 2007 and 2012 ice extents.

2001–05 and 2006–2010 showed the most pronounced change, as compared to the mean level of 34 years (Fig. 5).

For the period of 2001–05: (1) in winter months, the ice edge shifted 5 degrees northward along the western and eastern coasts of Greenland, so that the ice-pack no longer reached the southernmost coast of Greenland; (2) in summer months, ice extent shifted 1–3 degrees northward in nearly all sectors, with the most extreme shift occurring in the Greenland Sea. The ice edge did not change at the north coast of the Greenland and never expanded to the south of the archipelago of Svalbard; (3) in the freezing months (November and December), the ice recovery in Hudson Bay, Baffin Bay and the Greenland Sea tended to be less compared with previous years, mainly on account of oceanic currents and ice drift.

For the period of 2006–2010 (Fig. 5), summer ice-edge retreat was amplified: (1) during winter months, the ice edge shifted 1–3 degrees to the north in the Barents and Greenland seas (so the ice retreat occurred around Greenland in both winter and summer); and (2) in the summer months, a great retreat from the Pacific–Siberian sector occurred, with the ice edge shifting 4–5 degrees northward in the Chukchi, eastern Siberian and Laptev seas, and 2–4 degrees northward in the Kara Sea, Baffin Bay, Hudson Bay and the Canadian Arctic Archipelago.

To summarize, the Arctic sea-ice edge has been retreating during the last decade in the Atlantic sector in winter, and in the Pacific–Siberian sector in summer. For the Atlantic sector, the ice loss can be attributed to thinner sea ice from the Arctic and a strengthened and warmer Atlantic inflow. For the Pacific–Siberian sector, the extreme low summer ice extent in the last decade was coincident with the massive loss of the perennial ice (Comiso 2012).

Citation: *Polar Research* 2014, *33*, 21249, http://dx.doi.org/10.3402/polar.v33.21249

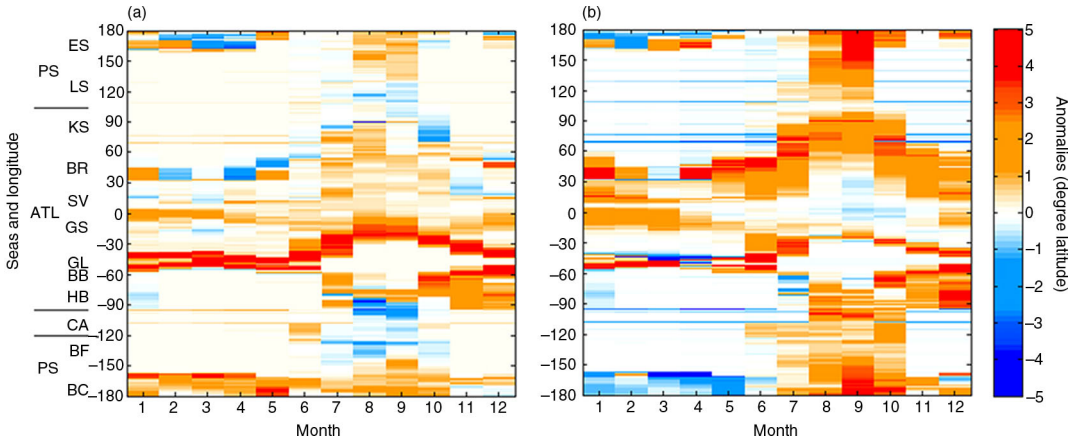

Fig. 5 (a) 2001–05 and (b) 2006–2010 monthly averaged latitudinal ice extent (degree) as compared to 34-year monthly mean. The following terms are abbreviated: eastern Siberian Sea (ES); Laptev Sea (LS); Kara Sea (KS); Barents Sea (BR); Svalbard (SV); Greenland Sea (GS); Greenland (GL); Baffin Bay (BB); Hudson Bay (HB); Canadian Arctic Archipelago (CA); Beaufort Sea (BF); Bering Sea/Chukchi Sea (BC); Pacific–Siberian sector (PS) and Atlantic sector (ATL).

Per-longitude changes in the magnitude of ice-edge retreat. The ice-edge latitudinal differences between winter maximum and summer minimum ice edges along each longitude degree in each year were compared with 34-year averaged winter/summer ice-edge latitudinal differences (Fig. 6). If this difference is higher than the 34-year mean level, it shows as a positive anomaly. The increasing difference (i.e., summer ice-edge retreat) is evident after the year of 2005 in nearly all sectors, except in Svalbard and the Greenland Sea. The northward shift of the ice edge is the highest in the Chukchi and eastern Siberian seas. This decline could be due to an increased warm Pacific Summer Water inflow, as reduced internal ice strength allowed a more efficient coupling of anticyclonic wind forcing to the upper ocean (Shimada et al. 2006). Another important mechanism contributing to the decline is the ice-albedo feedback (Perovich 2011), which further accelerated the ice melting during the Arctic summer.

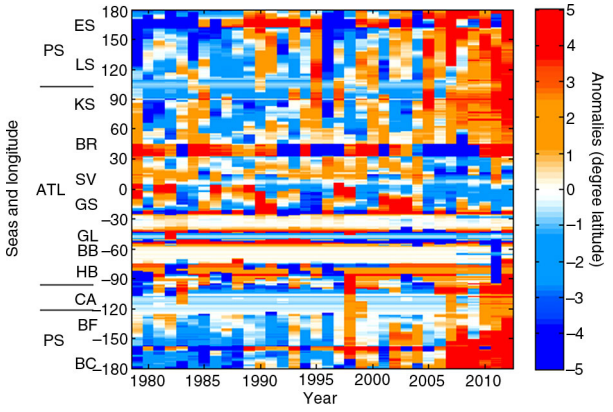

Fig. 6 Latitudinal ice edge difference (degree) between winter maximum and summer minimum as compared with 34-year mean difference for each longitude degree. The following terms are abbreviated: eastern Siberian Sea (ES); Laptev Sea (LS); Kara Sea (KS); Barents Sea (BR); Svalbard (SV); Greenland Sea (GS); Greenland (GL); Baffin Bay (BB); Hudson Bay (HB); Canadian Arctic Archipelago (CA); Beaufort Sea (BF); Bering Sea/Chukchi Sea (BC); Pacific–Siberian sector (PS) and Atlantic sector (ATL).

Trend of latitudinal ice edge

Trend of latitudinal ice edge per-longitude. The trend of Arctic ice-edge retreat is always anisotropic. This can be expressed by the slope of linear regression (Fig. 7) in each month and each integer degree of longitude. If the lower bounds of the 95% confidence

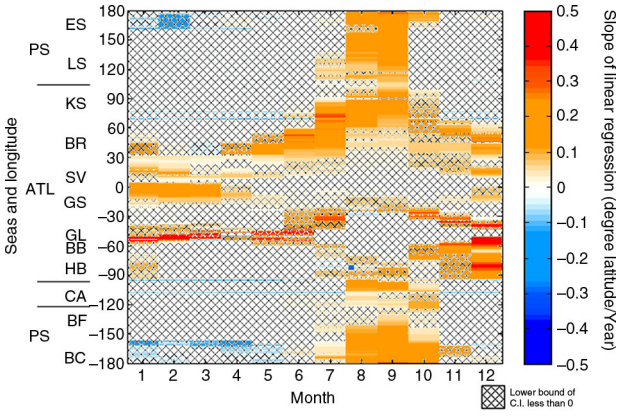

Fig. 7 Slope (degree/year) of 34-year linear trend per-longitude for each month, with insignificant trends marked with hatching. The following terms are abbreviated: eastern Siberian Sea (ES); Laptev Sea (LS); Kara Sea (KS); Barents Sea (BR); Svalbard (SV); Greenland Sea (GS); Greenland (GL); Baffin Bay (BB); Hudson Bay (HB); Canadian Arctic Archipelago (CA); Beaufort Sea (BF); Bering Sea/Chukchi Sea (BC); Pacific–Siberian sector (PS) and Atlantic sector (ATL).

Table 1 Slope of linear trend, confidence interval and coefficient of determination, for the 34-year latitudinal ice edge.

Geographic muting	Month	Slope of linear trend (degree/year)	Margins of error (degree/year)	Ratio of slope over margins of error	R^2
Excluded for winter	Jan	0.0559	±0.0310	1.8051	0.3197
	Feb	0.0371	±0.0243	1.5257	0.2869
	Mar	0.0318	±0.0253	1.2537	0.1896
	Apr	0.0216	±0.0327	0.6599	0.0621
Not excluded for other months	May	0.0156	±0.0143	1.0958	0.172
	Jun	0.0768	±0.0393	1.9541	0.398
	Jul	0.0581	±0.0203	2.8579	0.585
	Aug	0.0717	±0.0239	3.0009	0.609
	Sep	0.0898	±0.0276	3.2537	0.647
	Oct	0.0562	±0.0209	2.6864	0.564
	Nov	0.0405	±0.0209	1.937	0.402
	Dec	0.0545	±0.0215	2.5272	0.533

interval of these slopes are positive values, such changes tend to be a significant (0.05 significance level) northward trend, not random variation. If it is not significant, the ice-edge shift is most likely randomly varied. Only a few longitudes (particularly in cold months) show significantly advancing ice edge (i.e., southward trend) at a rate less than 0.2 degree/year. Most longitudes (particularly in warm months) show significantly retreating ice edge (northward trend) at rates 0.1–0.2 degree/year, with a few longitudes, particularly west of Greenland, showing 0.5 degree/year retreating. Fram Strait and the Greenland and western Barents seas show a 0.1–0.2 degree/year retreating trend in cold months. This could be partially attributed to the Atlantic water warming anomalies (Dmitrenko et al. 2008) and a stronger heat transport by ocean currents (like the West Spitsbergen Current)

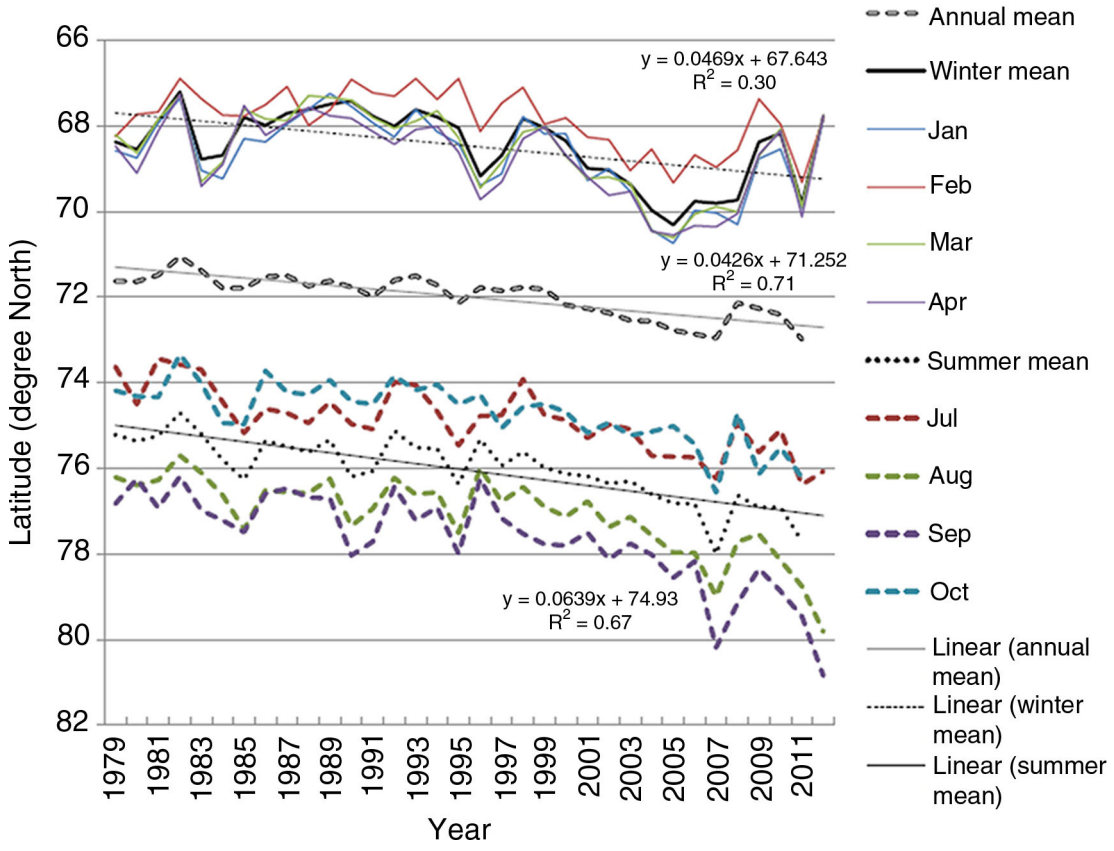

Fig. 8 Mean latitudinal ice edges in winter months, summer months and annually, and their linear trends.

Citation: *Polar Research* 2014, *33*, 21249, http://dx.doi.org/10.3402/polar.v33.21249

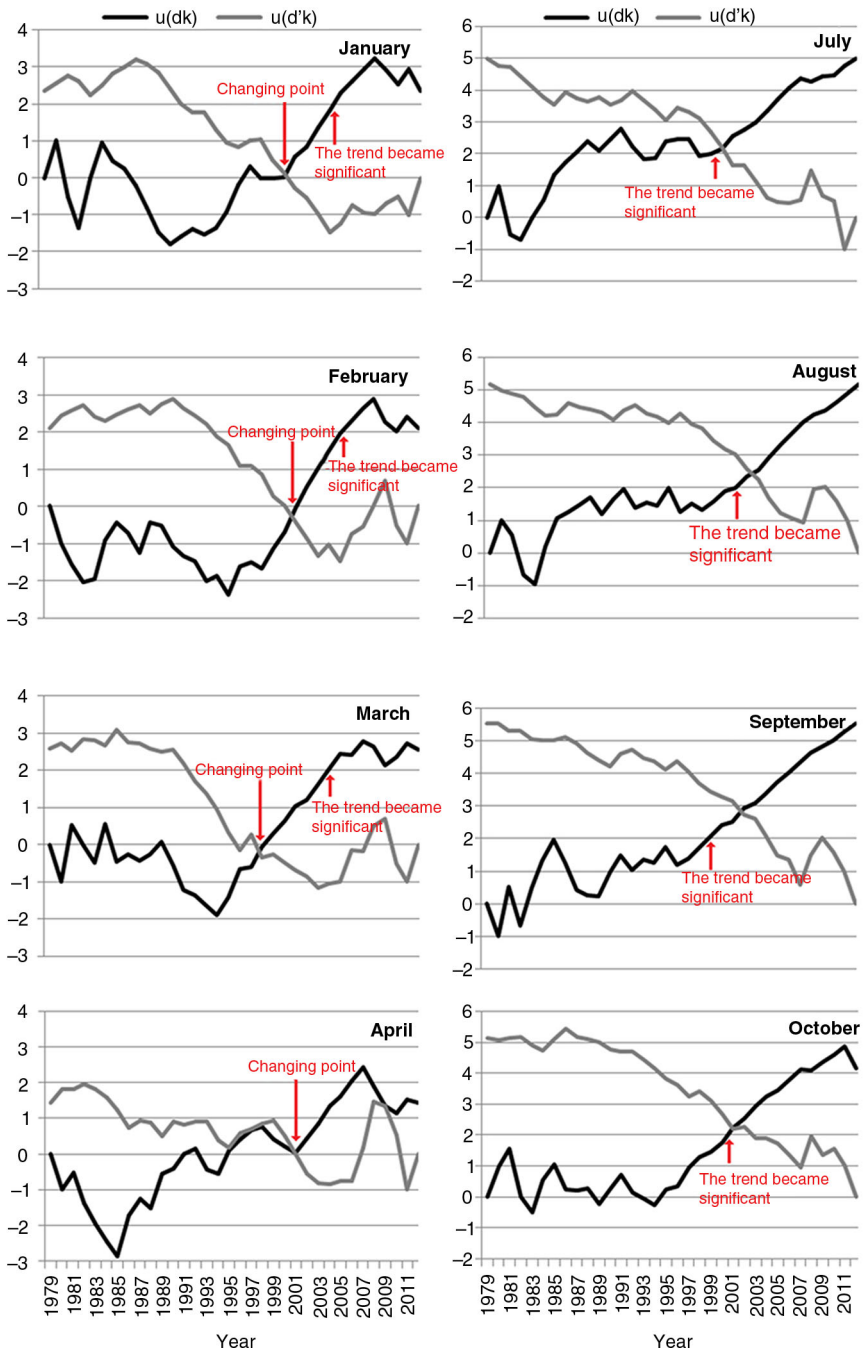

Fig. 9 Mann–Kendall change point detection in winter months and summer months.

through Fram Strait (Schauer et al. 2004). In the cold months, a 0.5 degree/year retreating trend occurred to the west of Greenland. In May, June and July, a 0.1–0.5 degree/year ice-edge retreating trend can be seen in the Barents Sea. In August, September and October, a >0.1 degree/year retreating trend occurred across the Pacific–Siberian sectors. The summer retreating trend in the East Siberian Sea and Chukchi Sea was the strongest, exceeding 0.2 degree/year in September. In the November and December, a 0.1–0.5 degree/year retreating trend can be seen in different areas of the Atlantic sector.

The winter retreating trend in the Baffin Bay, the Greenland Sea and the eastern Barents Sea indicates that the winter ice expansion is slowing in those sectors and the winter ice extent is declining. In summer, these areas show no significant trend since these areas are filled

with out-flowing sea ice, and the ice-edge variation is not obvious in summer.

As the anomalies of dynamic forcing do not keep a consistent trend, the retreating trend should be expressing the weakening ice strength (Tietsche et al. 2011). The ice edge in the Pacific–Siberian sector does not express a significant winter trend, but a significant summer retreating trend occurred in the entire sector in summer. This means that the seasonal oscillation is much stronger in the Pacific–Siberian sector than the Atlantic sector. Such oscillation is amplified by the long-wave negative feedback in winter and ice-albedo feedback in summer, as large areas of open water in summer enhance both thermodynamic and dynamic processes.

Trend of averaged latitudinal ice edge at all longitudes. The averaged latitudinal ice edges in all longitudes in each month all showed a decreasing (northward) trend (Table 1). This trend is much stronger in summer months (0.0562–0.0898 degree/year, across all directions) than in winter months (0.0216–0.0559 degree/year, with geographically muted areas excluded). The coefficients of determination (R^2) range from 0.56 to 0.65 in summer months. This indicates a near-linear change. For winter months, the coefficients of determination are less than 0.32, so the change in winter were not likely linear, and the trend is not so obvious.

Figure 8 shows the time series and linear trends of the latitudinal ice edge averaged for the winter months, summer months and yearly. The trend slope of summer mean ice edge (0.0639 degree/year) is larger than that of winter (0.0469 degree/year), with both larger than the annual mean (0.0426 degree/year). The ice edge in winter showed higher variations in January, March and April. The February has a lower variation and a further southward expanded ice edge. Time series of the annual mean eliminates such variation, showing a higher coefficient of determination ($R^2 = 0.71$), i.e., a better fitting linear trend.

Changing point of trend. The M–K procedure applied to the four winter months indicate that the changing points (years) of the trend in sea-ice extent are January and April in 2000, February in 2001 and March in 1998 (Fig. 9). Before the changing point (month/year), the trend was not pronounced and not significant (Table 2). The northward trend became significant in 2005 for January and February, 2004 for March and 2006 for April, at significance level of 0.05 (Fig. 9). Tests for the summer months (Fig. 9) indicate that the northward trend became significant in July 1999, August 2001, September 1999 and October 2000. As the value of changing point for these 4 months all exceeded the 95% confidence interval (>1.96) of the $u(d_k)$ statistics, they are therefore not the confirmed changing points; instead, the trend became more and more significant after the year 1999, and the probability of such a change being a random variation became extremely low.

Discussion and conclusion

Interpretation of Arctic sea-ice extent from a latitudinal ice-edge perspective can provide detailed information about ice-edge shifts in each direction. This method can objectively reveal the change of ice edge and is not be limited by geographic subsectors or regions, as has previously been done (Eisenman 2010; Cavalieri & Parkinson 2012). In addition, statistical inference and trend analysis are applied at each longitude, allowing analyses along each of 360 integer longitude directions.

In the 34 years examined, the onset of summer melt occurred earlier, the ice-edge changes became more rapid and the declining trend of summer minimum extent is evident. With the Arctic summer minimum sea-ice extent reaching the lowest point on record several times in recent years, especially 2007 and 2012, the declining trend has strengthened. Although the decline of the winter maximum extent is much smaller compared to that of the summer minimum extent, there has been a long-term declining trend in winter sea-ice extent. Winter inter-annual differences occurred only at the

Table 2 Slope of linear trend, confidence interval and coefficient of determination, for the years before the changing points of trends (winter, January–April), or before the years that the trend became significant (summer, July–August).

Month	Year	Slope of linear trend (degree/year)	Margins of error (degree/year)	Ratio of slope over margins of error	R^2
Jan	1979–2000	−0.0007	±0.0257	−0.0265	0
Feb	1979–2001	−0.0046	±0.0165	−0.2792	0.02
Mar	1979–1998	−0.0019	±0.0292	−0.0663	0
Apr	1979–2000	0.0019	±0.0240	0.0792	0
Jul	1979–2005	0.0424	±0.0545	0.7782	0.18
Aug	1979–2005	0.028	±0.0362	0.7725	0.15
Sep	1979–2004	0.0334	±0.0513	0.6516	0.12
Oct	1979–2006	0.0184	±0.0359	0.5118	0.08

Citation: *Polar Research* 2014, *33*, 21249, http://dx.doi.org/10.3402/polar.v33.21249

Bering, Baffin and Greenland seas and the Canadian Arctic Archipelago. As the sea ice retreated after the winter maximum extent, inter-annual variation of the ice edge occurred at almost all longitudes in the summer minimum sea-ice extent, except the north coast of Greenland. In summer months, the northward/declining trend occurred at almost every longitude (direction), especially at the Barents, Kara, Laptev, eastern Siberian, Chukchi and Beaufort seas. The northward ice-edge retreat in the eastern Siberian Sea, the Chukchi Sea, and the Beaufort Sea accounts for most of the decline in the ice extent.

The ice edge around Baffin Bay and Fram Strait was mostly dominated by sea-ice efflux, especially in the decadal efflux anomaly around 1990–97 (Vinje 2001). In the 2000s, contrary to Vinje's prediction (2001), the ice-edge retreat continues. The continuous ice-edge retreat around Fram Strait should be attributed to the greater susceptibility of the thin ice to ice deformation and drift caused by shorter-term atmospheric changes (Zhang et al. 2012), and ice melt caused by a warmer West Spitsbergen Current.

The M–K non-parametric trend test suggests that the trend of decline became more significant since the year 1999 for the summer months, indicating that the decline has been accelerating. As long-wave negative feedback is constantly contributing to the ice-edge expansion in each fall/winter freezing months, there is not much observed decrease in winter sea-ice extent. However, the mechanical strength of sea ice is much lower due to the dynamic and thermodynamic mechanics mentioned before (like the continuous Arctic warming and the highly variable atmospheric and oceanic forcing). (Maslanik et al. 2007; Kwok et al. 2009).

The thinned sea-ice thickness and lowered mechanical strength (Perovich 2011) will finally lead to a massive ice-edge retreat. When the trend of ice extent decline became significant, the ice-albedo positive feedback and ice efflux anomalies take full effect, so the extremely low ice extent event in summer will be more frequent, resulting in more severe ice loss (Kinnard et al. 2011).

M–K statistics for winter months reveal the trend changing points around 2000, with significant trend since around 2005. This trend was weaker than the summer declining trend because the long-wave negative feedback became even stronger in the context of more rapid ice decline. The change was also highly variable and not likely linear, suggesting that atmospheric/oceanic forcing is dominating and, weakening ice cover recovery in winter. Most of the recovered ice cover did not survive the next summer, contributing little to the ice thickness accumulation and the multiyear ice replenishment (Vinnikov et al. 1999; Comiso et al. 2008; Cavalieri & Parkinson 2012; Stammerjohn et al. 2012). If Arctic warming persists, these positive feedbacks will be continuously in effect, extreme summer ice retreat events will be more common and we will be well on our way toward the ice-free Arctic summers that have been predicted (Holland et al. 2010).

Acknowledgements

This work was partially supported by the University of Texas at San Antonio Collaborative Research Seed Grant Program, the International Cooperation Program of Chinese Arctic and Antarctic Administration (no. IC201301), and the Chinese Polar Environment Comprehensive Investigation & Assessment Programs (no. CHINARE2013-04-03). Provision of ice index data through NSIDC is sincerely appreciated. Critical reviews and constructional comments from two anonymous reviewers to improve the quality of this manuscript are greatly appreciated.

References

Campbell W.J., Ramseier R.O., Zwally H.J. & Gloersen P. 1980. Arctic sea-ice variations from time-lapse passive microwave imagery. *Boundary-Layer Meteorology 18*, 99–106.

Cavalieri D.J., Gloersen P. & Campbell W.J. 1984. Determination of sea ice parameters with the NIMBUS 7 SMMR. *Journal of Geophysical Research—Atmospheres 89*, 5355–5369.

Cavalieri D.J. & Parkinson C.L. 2012. Arctic sea ice variability and trends, 1979–2010. *The Cryosphere 6*, 881–889.

Chapman W.L. & Walsh J.E. 1993. Recent variations of sea ice and air temperature in high latitudes. *Bulletin of the American Meteorological Society 74*, 33–47.

Comiso J.C. 1986. Characteristics of Arctic winter sea ice from satellite multispectral microwave observations. *Journal of Geophysical Research—Oceans 91*, 975–994.

Comiso J.C. 2003. Warming trends in the Arctic from clear sky satellite observations. *Journal of Climate 16*, 3498–3510.

Comiso J.C. 2012. Large decadal decline of the Arctic multiyear ice cover. *Journal of Climate 25*, 1176–1193.

Comiso J.C. & Kwok R. 1996. Surface and radiative characteristics of the summer Arctic sea ice cover from multisensor satellite observations. *Journal of Geophysical Research—Oceans 101*, 28397–28416.

Comiso J.C., Parkinson C.L., Gersten R. & Stock L. 2008. Accelerated decline in the Arctic sea ice cover. *Geophysical Research Letters 35*, L01703, doi: 10.1029/2007GL031972.

Divine, D.V. & Dick C. 2006. Historical variability of sea ice edge position in the Nordic seas. *Journal of Geophysical Research—Oceans 111*, C01001, doi: 10.1029/2004JC002851.

Dmitrenko I.A., Polyakov I.V., Kirillov S.A., Timokhov L.A., Frolov I.E., Sokolov V.T., Simmons H.L., Ivanov V.V. & Walsh D. 2008. Toward a warmer Arctic Ocean: spreading of the early 21st century Atlantic Water warm anomaly

along the Eurasian Basin margins. *Journal of Geophysical. Research—Oceans 113*, C05023, doi: 10.1029/2007JC004158.

Eisenman I. 2010. Geographic muting of changes in the Arctic sea ice cover. *Geophysical Research Letters 37*, L16501, doi: 10.1029/2010GL043741.

Emery W.J., Fowler C. & Maslanik J. 1994. Arctic sea ice concentrations from special sensor microwave imager and advanced very high resolution radiometer satellite data. *Journal of Geophysical Research—Oceans 99*, 18329–18342.

Fetterer F. 2002–2012. *Sea ice index*. Digital media. National Snow and Ice Data Center. Boulder: University of Colorado.

Fetterer F. & Knowles K. 2004. Sea ice index monitors polar ice extent. *Eos, Transactions of the American Geophysical Union 85*, 163–163.

Fetterer F. & Untersteiner N. 1998. Observations of melt ponds on Arctic sea ice. *Journal of Geophysical Research—Oceans 103*, 24821–24835.

Gillett N.P., Allen M., McDonald R., Senior C., Shindell D. & Schmidt G. 2002. How linear is the Arctic Oscillation response to greenhouse gases? *Journal of Geophysical Research—Atmospheres 107*, article no. 4022, doi: 10.1029/2001JD000589.

Gloerson P. & Campbell W.J. 1991. Recent variations in Arctic and Antarctic sea-ice covers. *Nature 352*, 33–36.

Haas C., Pfaffling A., Hendricks S., Rabenstein L., Etienne J. & Rigor I. 2008. Reduced ice thickness in Arctic Transpolar Drift favors rapid ice retreat. *Geophysical Research Letters 35*, L17501, doi: 10.1029/2008GL034457.

Hansen J., Ruedy R., Sato M. & Lo K. 2010. Global surface temperature change. *Reviews of Geophysics 48*, RG4004, doi: 10.1029/2010RG000345.

Hansen J., Sato M., Ruedy R., Lo K., Lea D.W. & Medina-Elizade M. 2006. Global temperature change. *Proceedings of the National Academy of Sciences 103*, 14288–14293.

Holland M.M., Serreze M.C. & Stroeve J. 2010. The sea ice mass budget of the Arctic and its future change as simulated by coupled climate models. *Climate Dynamics 34*, 185–200.

Hollinger J.P., Peirce J.L. & Poe G.A. 1990. SSM/I Instrument Evaluation. *IEEE Transactions on Geoscience and Remote Sensing 28*, 781–790.

Jeffries M.O., Overland J.E. & Perovich D.K. 2013. The Arctic shifts to a new normal. *Physics Today 66*, 35–40.

Kendall M. 1955. *Rank correlation methods*. New York: Hafner Publishing Co.

Kinnard C., Zdanowicz C., Fisher D., Isaksson E., Vernal A. & Thompson L. 2011. Reconstructed changes in Arctic sea ice over the past 1,450 years. *Nature 479*, 509–512.

Kwok R. 2002. Sea ice concentration estimates from satellite passive microwave radiometry and openings from SAR ice motion. *Geophysical Research Letters 29*, article no. 1311, doi: 10.1029/2002GL014787.

Kwok R., Cunningham G.F., Wensnahan M., Rigor I., Zwally H.J. & Yi D. 2009. Thinning and volume loss of the Arctic Ocean sea ice cover: 2003–2008. *Journal of Geophysical Research—Oceans 114*, C07005, doi: 10.1029/2009JC005312.

Mahoney A.R., Barry R.G., Smolyanitsky V. & Fetterer F. 2008. Observed sea ice extent in the Russian Arctic, 1933–2006. *Journal of Geophysical Research—Oceans 113*, C11005, doi: 10.1029/2008JC004830.

Manak D.K. & Mysak L.A. 1987. Climatic atlas of Arctic sea ice extent and anomalies, 1953–1984. *Climate Research Group Report 87–8*. Montréal: McGill University.

Mann H.B. 1945. Nonparametric tests against trend *Econometrica 13*, 245–259.

Maslanik J., Drobot S., Fowler C., Emery W. & Barry R. 2007. On the Arctic climate paradox and the continuing role of atmospheric circulation in affecting sea ice conditions. *Geophysical Research Letters 34*, L03711, doi: 10.1029/2006GL028269.

Mauritzen C. & Häkkinen S. 1997. Influence of sea ice on the thermohaline circulation in the Arctic–North Atlantic Ocean. *Geophysical Research Letters 24*, 3257–3260.

Meier W., Stroeve J., Fetterer F. & Knowles K. 2005. Reductions in Arctic sea ice cover no longer limited to summer. *Eos, Transactions of the American Geophysical Union 86*, 326–326.

Ogi M. & Wallace J.M. 2007. Summer minimum Arctic sea ice extent and the associated summer atmospheric circulation. *Geophysical Research Letters 34*, L12705, doi: 10.1029/2007GL029897.

Overland J., Turner J., Francis J., Gillett N., Marshall G. & Tjernström M. 2008. The Arctic and Antarctic: two faces of climate change. *Eos, Transactions of the American Geophysical Union 89*, 177–178.

Parkinson C.L. & Cavalieri D.J. 2008. Arctic sea ice variability and trends, 1979–2006. *Journal of Geophysical Research—Oceans 113*, C07003, doi: 10.1029/2007JC004558.

Parkinson C.L., Cavalieri D.J., Gloersen P., Zwally H.J. & Comiso J.C. 1999. Arctic sea ice extents, areas, and trends, 1978–1996. *Journal of Geophysical Research—Oceans 104*, 20837–20856.

Parkinson C.L. & Comiso J.C. 2013. On the 2012 record low Arctic sea ice cover: combined impact of preconditioning and an August storm. *Geophysical Research Letters 40*, 1356–1361.

Partington K., Flynn T., Lamb D., Bertoia C. & Dedrick K. 2003. Late twentieth century Northern Hemisphere sea-ice record from U.S. National Ice Center ice charts. *Journal of Geophysical Research—Oceans 108*, article no. 3343, doi: 10.1029/2002JC001623.

Perovich D.K. 2011. The changing Arctic sea ice cover. *Oceanography 24*, 162–173.

Perovich D.K., Grenfell T.C., Light B. & Hobbs P.V. 2002. Seasonal evolution of the albedo of multiyear Arctic sea ice. *Geophysical Research Letters 107*, article no. 8044, doi: 10.1029/2000JC000438.

Rigor I.G., Wallace J.M. & Colony R.L. 2002. Response of sea ice to the Arctic Oscillation. *Journal of Climate 15*, 2648–2663.

Schauer, U., Fahrbach E., Osterhus S. & Rohardt G. 2004. Arctic warming through the Fram Strait: oceanic heat transport from 3 years of measurements. *Journal of Geophysical Research—Oceans 109*, C06026, doi: 10.1029/2003JC001823.

Serreze M.C., Maslanik J.A., Scambos T.A., Fetterer F., Stroeve J., Knowles K., Fowler C., Drobot S., Barry R.G. & Haran T.M. 2003. A record minimum arctic sea ice extent and area in 2002. *Geophysical Research Letters 30*, article no. 1110, doi: 10.1029/2002GL016406.

Shakun J.D., Clark P.U., He F., Marcott S.A., Mix A.C., Liu Z., Otto-Bliesner B., Schimittner A. & Bard E. 2012. Global warming preceded by increasing carbon dioxide concentrations during the last deglaciation. *Nature 484*, 49–54.

Shimada K., Kamoshida T., Itoh M., Nishino S., Carmack E., McLaughlin F.A., Zimmermann S. & Proshutinsky A. 2006. Pacific Ocean inflow: influence on catastrophic reduction of sea ice cover in the Arctic Ocean. *Geophysical Research Letters 33*, L08605, doi: 10.1029/2005GL025624.

Stammerjohn S., Massom R., Rind D. & Martinson D. 2012. Regions of rapid sea ice change: an inter-hemispheric seasonal comparison. *Geophysical Research Letters 39*, L06501, doi: 10.1029/2012GL050874.

Tietsche S., Notz D., Jungclaus J.H. & Marotzke J. 2011. Recovery mechanisms of Arctic summer sea ice. *Geophysical Research Letters 38*, L02707, doi: 10.1029/2010GL045698.

Vinje T. 2001. Fram Strait ice fluxes and atmospheric circulation: 1950–2000. *Journal of Climate 14*, 3508–3517.

Vinnikov K.Y., Robock A., Stouffer R.J., Walsh J.E., Parkinson C.L., Cavalieri D.J., Mitchell J.F.B., Garrett D. & Zakharov V.F. 1999. Global warming and Northern Hemisphere sea ice extent. *Science 286*, 1934–1937.

Wang Y.H., Magnusdottir G., Stern H., Tian X. & Yu Y. 2012. Decadal variability of the NAO: introducing an augmented NAO index. *Geophysical Research Letters 39*, L21702, doi: 10.1029/2012GL053413.

Xie H., Lei R., Ke C., Wang H., Li Z., Zhao J. & Ackely S.F. 2013. Summer sea ice characteristics and morphology in the Pacific Arctic sector as observed during the CHINARE 2010 cruise. *The Cryosphere 7*, 1057–1072.

Zhang J., Lindsay R., Schweiger A. & Rigor I. 2012. Recent changes in the dynamic properties of declining Arctic sea ice: a model study. *Geophysical Research Letters 39*, L20503, doi: 10.1029/2012GL053545.

Zhang J., Lindsay R., Schweiger A. & Steele M. 2013. The impact of an intense summer cyclone on 2012 Arctic sea ice retreat. *Geophysical Research Letters 40*, 720–726.

Zhang J., Lindsay R., Steele M. & Schweiger A. 2008. What drove the dramatic retreat of Arctic sea ice during summer 2007? *Geophysical Research Letters 35*, L11505, doi: 10.1029/2008GL034005.

Zhang J. & Rothrock D.A. 2003. Modeling global sea ice with a thickness and enthalpy distribution model in generalized curvilinear coordinates. *Monthly Weather Review 131*, 245–259.